Chapter 5

Role of Ca off-Centering in Tuning Ferroelectric Phase Transitions in $Ba(Zr,Ti)O_3$System

Desheng Fu and Mitsuru Itoh

Additional information is available at the end of the chapter

http://dx.doi.org/10.5772/61017

Abstract

We here report the substitution effects of the smaller Ca for the bulky Ba in the $(Ba_{1-x}Ca_x)(Ti_{-1-y}Zr_y)O_3$ perovskite oxides for two systems $(Ba_{1-x}Ca_x)TiO_3$ with y=0 and $(Ba_{1-x}Ca_x)(Ti_{0.9}Zr_{0.1})O_3$ with y=0.1. Ca off-centering was found to play a critical role in stabilizing the ferroelectric phase and tuning the polarization states in both systems. It was demonstrated that the atomic displacement due to Ca off-centering in the bulky Ba-sites in the perovskite structure provides an effective approach to compensate for the reduction of ferroelectricity due to chemical pressure, which allows to keep the Curie point nearly constant in the $(Ba_{1-x}Ca_x)TiO_3$ system and increase the Curie point in the $(Ba_{1-x}Ca_x)(Ti_{0.9}Zr_{0.1})O_3$ system. It was commonly observed that the Ca off-centering effects lead to the shift of the rhombohedral–orthorhombic and orthorhombic–tetragonal phase transitions toward lower temperatures and the ferroelectric stability of the tetragonal phase, resulting in the occurrence of quantum phase transitions with interesting physical phenomena at low temperatures in the $(Ba_{1-x}Ca_x)TiO_3$ system and remarkable enhancement of electromechanical coupling effects around room temperature in the $(Ba_{1-x}Ca_x)(Ti_{0.9}Zr_{0.1})O_3$ systems over a wide range of Ca-concentrations. These findings may be of great interest for the design of green piezoelectric materials.

Keywords: Ca off–centering, $BaTiO_3$, $Ba(Zr,Ti)O_3$, perovskite oxides, ferroelectric, piezoelectric, phase transition, quantum effects, electromechanical coupling effects

1. Introduction

There is increased interest in developing green piezoelectric materials in the field of electronics due to environmental concerns regarding the Pb-toxicity in commercially used lead-based $Pb(Zr,Ti)O_3$ (PZT) piezoelectric ceramics. As listed in Table 1 (Ref. 1-4), $BaTiO_3$ single crystals have the highest piezoelectric coefficients among single crystals of lead-free piezoelectrics. Although the reported values of its piezoelectric coefficient vary somewhat, recent investigations on the mono-domain of a single crystal by high energy synchrotron x-ray radiation show that $BaTiO_3$ has a d_{33} value of 149±54 pm/V at least at the level of lattice distortion (Fig. 1).[4] The large piezoelectric response makes $BaTiO_3$ a promising material for novel green piezoelectric ceramics.[5-9]

Crystal	Point group	d_{33} (pC/N)	ε_{33}	k (%)
quartz	32	2.3(d_{11})	4.6	10 (X-cut)
ZnO	6mm	10.6	11	41 (k_{33})
$LiNbO_3$	3m	6	30	17 (Z-cut)
$PbTiO_3$	4mm	19.3	121	64(k_{33})
$BaTiO_3$	4mm	149	168	65(k_{33})
PZN-PT8%	3m[111] [001]	84 2500	1000 5000	0.39(k_{33}) 0.94(k_{33})

Table 1. Typical piezoelectric crystals and their piezoelectric (d_{33} or d_{11}) & dielectric (ε_{33}) constants, and electromechanical coupling factor k.[1-4]

Piezoelectricity is the ability of a single crystal with non-centrosymmetry (with the exception of point group 432) to develop an electric charge proportional to a mechanical stress or to produce a deformation proportional to an electric field. The piezoelectricity in $BaTiO_3$ is a direct result of its ferroelectricity, originating from the Ti atomic displacement in the oxygen octahedron of the ABO_3 perovskite structure[10, 11] (Fig. 2). As can be inferred from the depiction of the variation of the dielectric permittivity with temperature in Fig. 2, there are two challenging issues that remain to be solved for $BaTiO_3$: (1) the temperature instability of physical properties around room temperature due to the tetragonal (T)-orthorhombic (O) phase transition; and (2) its relatively lower Curie point of ~400 K in comparison with lead-based piezoelectrics. A-site substitution of Pb for Ba is able to increase the Curie point; however, such an approach is undesirable for green piezoelectrics. Principally, A-site and/or B-site substitution can be used to modify the ferroelectricity of $BaTiO_3$. Here, we show that A-site substitution of Ca for Ba in the Ba-based perovskite oxides can lead to a variety of interesting phenomena: (1) the dramatic improvement of temperature stability of its physical properties, (2) the occurrence of quantum fluctuation at low temperatures, and (3) remarkable enhancement of electromechanical responses.[6-9]

http://dx.doi.org/10.5772/61017

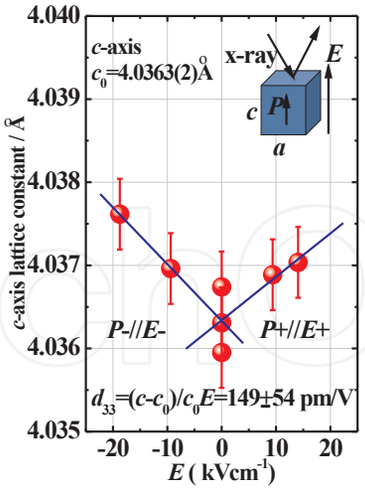

Figure 1. Lattice distortion of mono-domain of a $BaTiO_3$ crystal under the application of an electric field.[4]

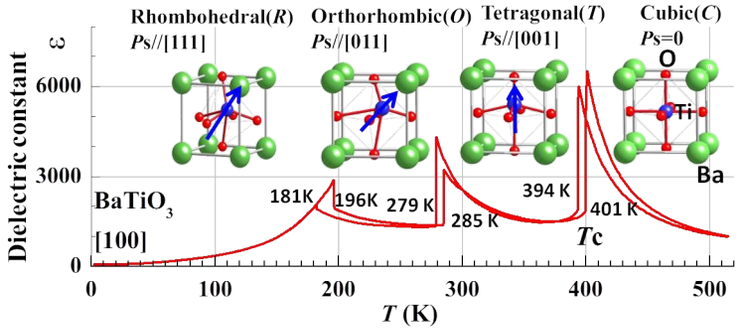

Figure 2. Change with temperature of the dielectric permittivity of a $BaTiO_3$ single crystal. The schematics of Ti displacement in the oxygen octahedron of the perovskite structure are also shown.

2. Effects of Ca substitution in $BaTiO_3$

In the early years of 1960, Mitsui and Westphal investigated the influence of Ca substitution on the phase transitions in $BaTiO_3$.[12] Using the ceramic samples, they established a phase diagram of $(Ba_{1-x}Ca_x)TiO_3$ in the composition range of x<0.25 mole for temperatures higher than ~100 K. One interesting finding is that the Curie point remained nearly unchanged within the studied composition range. Such behavior is unexpected when considering that $CaTiO_3$ is paraelectric and that the ionic radius of Ca (~1.34Å) is smaller than that of Ba (~1.60Å),[13] which would lead to the shrinkage of the unit cell and a reduction in ferroelectricity of systems with substitution of Ca for Ba. To gain new insight into the role of Ca substitution in Ba-based perovskite oxides, we re-examined the $(Ba_{1-x}Ca_x)TiO_3$ system using single crystal samples, which allowed us to observe the intrinsic phenomena of the system.[6-8, 14]

2.1. Crystal growth

To obtain a single crystal of $(Ba_{1-x}Ca_x)TiO_3$, we used the floating zone (FZ) technique (Fig. 3(a)) that allowed us to grow a single crystal with high purity. According to the reported phase equilibria in the system $(1-x)BaTiO_3$-$xCaTiO_3$ (Fig. 4), only the crystal with a congruent melting composition (x=0.27 report by DeVries and Roy[15] or x=0.227 report by Kuper et al.[16]) can be directly grown from the melt. Surprisingly, using the FZ technique, we could grow a single crystal of $(Ba_{1-x}Ca_x)TiO_3$ with a perovskite structure for a wide composition range of $0.02 \leq x \leq 0.34$ with a high growth rate of 20 mm/h.[6] Fig. 3(b) shows a rod of crystal obtained by this method. It was found that the crystal can be stably grown under an atmosphere of Ar or N_2 gas. The crystal was yellowish but transparent. The Laue X-ray diffraction patterns clearly indicated that the obtained $(Ba_{1-x}Ca_x)TiO_3$ crystal had a perovskite structure.

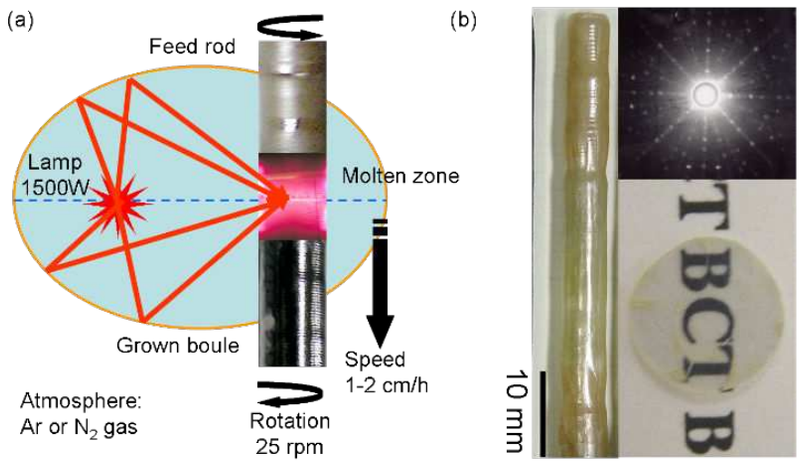

Figure 3. (a)A schematic drawing of the floating zone (FZ) technique used to grow the $(Ba_{1-x}Ca_x)TiO_3$ single crystal. (b) Photograph of the $(Ba_{1-x}Ca_x)TiO_3$ single crystal grown by the FZ technique and its Laue X-ray back diffraction patterns along the $[001]_c$ direction of the perovskite structure.

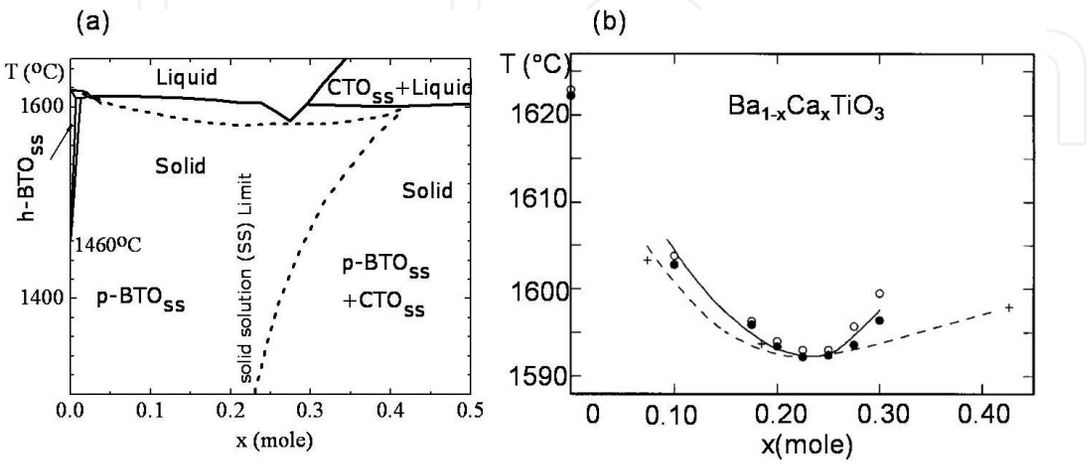

Figure 4. Phase equilibria in the system $(1-x)BaTiO_3$-$xCaTiO_3$ reported by (a) DeVries and Roy[15] and (b) Kuper et al.[16]

http://dx.doi.org/10.5772/61017

2.2. Dielectric behaviors

Figure 5 shows the temperature dependence of the dielectric permittivity of a $(Ba_{1-x}Ca_x)TiO_3$ single crystals in the temperature range from 2K to 400K. Compared with the polycrystalline ceramics, the $(Ba_{1-x}Ca_x)TiO_3$ single crystal showed a very sharp change of dielectric response at the phase transition, allowing easy determination of the transition temperatures. Similar to the polycrystalline ceramics[12], the Curie point was nearly independent of the Ca concentration. However, the *T*–*O* and *O*-rhombohedral (*R*) ferroelectric transitions shifted to lower temperatures as the Ca concentration increased. For compositions of x>0.23, these two transitions completely disappeared, and the *T*-phase was the only stable ferroelectric phase in the crystal. This situation is very similar to that of $PbTiO_3$, in which the *T*-phase is the only stable ferroelectric structure. Another interesting finding was that the dielectric permittivity was nearly unchanged for temperatures lower than the Curie point for x>0.23. This unique behavior provides the possibility of designing electronic devices that operate stably in a wide temperature range from the boiling point of water all the way down to absolute zero Kelvin using $(Ba_{1-x}Ca_x)TiO_3$.

As is well known, the dielectric response in displacive-type ferroelectrics is dominated by phonon dynamics, particularly the soft-mode behavior. Lyddane–Sachs–Teller (LST) relationship predicts that the dielectric permittivity is inversely proportional to the soft-mode frequency. As a step toward understanding the temperature independence of the dielectric response of $(Ba_{1-x}Ca_x)TiO_3$ (x >0.23), we performed confocal micro-Raman scattering measurements for the $(Ba_{1-x}Ca_x)TiO_3$ (x =0.233) single crystals to clarify its soft-mode dynamics.[14] In contrast to $BaTiO_3$, a well-defined soft phonon mode was observed for temperatures lower than the Curie point in the $(Ba_{1-x}Ca_x)TiO_3$ (x =0.233) single crystals. The temperature dependence of the soft-mode frequency agreed qualitatively with the dielectric permittivity through the Lyddane–Sachs–Teller relationship (Fig. 6). This result clearly indicates that the unique dielectric response of $(Ba_{1-x}Ca_x)TiO_3$ (x=0.233) is directly derived from its soft-mode dynamics.

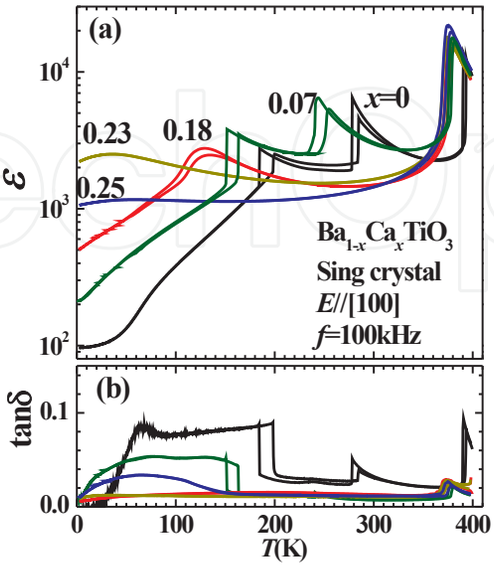

Figure 5. Dielectric behaviors of $(Ba_{1-x}Ca_x)TiO_3$ single crystals.

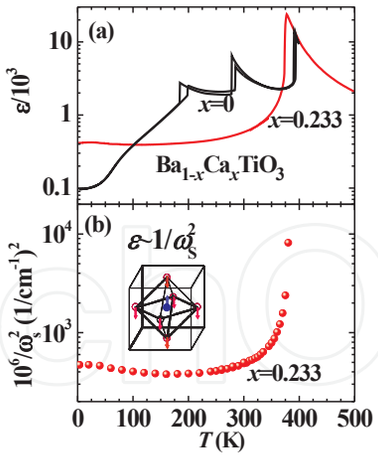

Figure 6. Comparison of (a) dielectric permittivity of $(Ba_{1-x}Ca_x)TiO_3$ single crystals and (b) the phonon frequency of the Slater soft-mode.

2.3. Phase diagram and quantum phase transitions

From the temperature change of dielectric permittivity of a $(Ba_{1-x}Ca_x)TiO_3$ crystal, we have established its phase diagram in a composition range of $x \leq 0.34$ for temperature down to 2 K (Fig. 7). Compared with the phase diagram proposed by Mitsui and Westphal for ceramics,[12] our phase diagram has been expanded to a composition up to x=0.34 mole and to temperatures as low as 2 K. These expansions of composition and temperature allow us to reveal some unexpected phenomena in this system: (1) ferroelectric *R*- and *O*-phases become unstable as the Ca concentration increased, and they are predicted to disappear at $x>x_c^{O\text{-}R}$ =0.18 and $x>x_c^{T\text{-}O}$=0.233, respectively; and (2) the ferroelectric *T*-phase is a ground state for $x> x_c^{T\text{-}O}$.

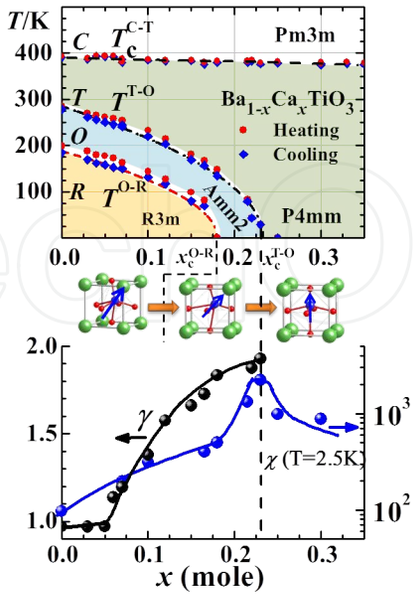

Figure 7. Top panel: phase diagram of $(Ba_{1-x}Ca_x)TiO_3$ crystals. Left of bottom panel: Change of critical exponent γ for the dielectric susceptibility in the *T-O* phase transition with the composition. Right of bottom panel: Variation of the dielectric susceptibility measured at 2.5 K with the composition.

http://dx.doi.org/10.5772/61017

One important finding is that ferroelectric–ferroelectric quantum phase transitions occur in $(Ba_{1-x}Ca_x)TiO_3$ crystals. The occurrence of ferroelectric–ferroelectric quantum phase transitions is supported by two experimental facts: the compositional dependence of $T^{O\text{-}R}$ and $T^{T\text{-}O}$ transition temperatures and the temperature dependence of the dielectric susceptibility in the crystals at compositions close to $x_c^{T\text{-}O}$. The theoretical and experimental studies[17-19] on quantum phase transitions indicate that (a) for a quantum ferroelectric, the transition temperature depends on the substitution concentration (i.e., on an effective order parameter) as

$$T_c \propto \left(x - x_c\right)^{1/2}, \tag{1}$$

as opposed to the classical relationship,

$$T_c \propto \left(x - x_c\right). \tag{2}$$

(b) The inverse dielectric susceptibility varies with temperature as

$$\chi^{-1} \propto \left(T - T_c\right)^2 \tag{3}$$

for the quantum mechanical limit instead of the classical Curie law

$$\chi^{-1} \propto \left(T - T_c\right). \tag{4}$$

Our phase diagram clearly shows that the *T-O* and *O-R* phase transitions deviate from the classical relationship (equation (2)) for $x \leq 0.06$, and exactly follow equation (1) for $x > 0.06$ with x_c equal to $x_c^{T\text{-}O}=0.233$ and $x_c^{O\text{-}R}=0.18$, respectively.

To examine point (b), we have analyzed the temperature variation of the inverse dielectric susceptibility of *T-O* phase transition in the $(Ba_{1-x}Ca_x)TiO_3$ crystals with the following equation,

$$\chi^{-1} \propto \left(T - T_c\right)^{\gamma}. \tag{5}$$

Figure 8 shows two typical examples: one for $x=0$ and another for $x=0.23$ close to $x_c^{T\text{-}O}$. For pure $BaTiO_3$ with $x=0$, the classical Curie law with $\gamma=1$ was observed to be operative. In contrast, for $x=0.23$, the critical exponent γ for the susceptibility was found to have a value of 2, which is predicted for the quantum phase transition (equation (3)). The left of the bottom panel in Fig. 7 shows the variation of γ with x. It is clear that the γ value changes from the value of the classical limit to that of the quantum limit as x increases from 0 to $x_c^{T\text{-}O}$. This fact again indicates that a quantum phase transition indeed occurs at zero Kelvin in the system when the Ca

concentration increases. Interestingly, a dielectric anomaly was observed for the *T-O* quantum phase transition at $x = x_c^{T\text{-}O}$ as shown at the right of the bottom panel of Fig. 7. At a temperature of 2.5 K, close to zero Kelvin, the crystal with x=0.23 close to $x_c^{T\text{-}O}$ shows a maximum value of dielectric susceptibility in the system.

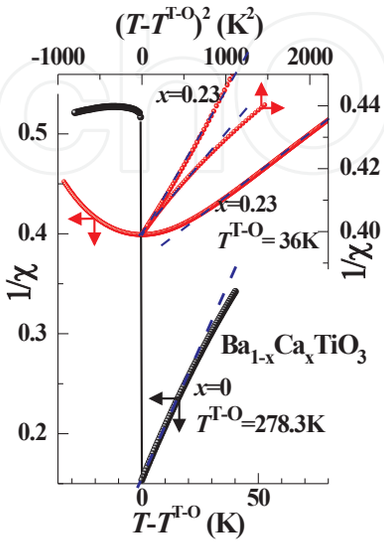

Figure 8. Change of the inverse dielectric susceptibility (χ=ε-1) near the *T-O* phase transition in $(Ba_{1-x}Ca_x)TiO_3$ crystals.

2.4. Ca off-centering predicted from first principles calculations

As mentioned above, the ionic radius of Ca is approximately 16% smaller than that of Ba. The substitution of Ca for Ba will absolutely result in the shrinkage of the perovskite unit cell. As shown in Fig. 9(a), both *a*- and *c*-axes of the tetragonal structure shrink with increasing Ca concentration, resulting in the reduction of the unit cell. The volume of the unit cell of x=0.34 is approximately 3.6% smaller than that of pure $BaTiO_3$. This chemical-pressure-induced reduction of the unit cell does not have significant influence on the Curie point ($T_c^{C\text{-}T}$) of the system (Fig. 9(c)).

In contrast, for the case of hydrostatic pressure, at the same level of unit-cell reduction, the Curie point is reduced to ~180 K, which is greatly lower than the ~400 K of pure $BaTiO_3$ (Fig. 9(c)). The hydrostatic pressure gradually reduces the Curie point, leading to the complete disappearance of ferroelectricity in $BaTiO_3$ at a level of 5% reduction of the unit cell. Although the chemical substitution of the smaller Ca for the bulky Ba also leads to the reduction of the unit cell, the effects of chemical pressure on the ferroelectricity in the $(Ba_{1-x}Ca_x)TiO_3$ system were very different from what we would expect with the application of hydrostatic pressure.

Apparently, the reduction of the unit cell by the chemical pressure shrinks the oxygen octahedron in the perovskite structure, resulting in the reduction of available space for a Ti off-centering shift in the oxygen octahedron. Since the ferroelectricity is derived from the Ti-shift in the oxygen octahedron in the perovskite structure of $BaTiO_3$, it is naturally expected that chemical-pressure-induced reduction of the unit cell in the $(Ba_{1-x}Ca_x)TiO_3$ system should

http://dx.doi.org/10.5772/61017

weaken the ferroelectricity of the system and result in a decrease in its Curie point. However, as shown in the phase diagram in Fig. 7 and Fig. 9, the Curie point remains nearly unchanged with the Ca substitution. Also, as shown in Fig. 9(b), the tetragonality (*c*/*a*), which is generally used to estimate the atomic displacement and thus the ferroelectricity and polarization in the tetragonal ferroelectric,[20, 21] maintains a constant value in the whole composition range in the $(Ba_{1-x}Ca_x)TiO_3$ system. In accordance with such unchanged tetragonality, we observed that the saturation polarization is also nearly independent on the Ca substitution within the limits of a solid solution (see Fig. 11).[8] These facts suggest that in addition to the Ti displacement in the oxygen octahedron, there should be an additional atomic displacement to contribute to the ferroelectricity of the $(Ba_{1-x}Ca_x)TiO_3$ system. The ionic radii of Ca and Ba are 1.34 Å and 1.61 Å, respectively. There is a difference of 0.27 Å between them. This suggests that the smaller Ca ion may have an off-centering displacement in the bulky Ba sites (Fig. 10(b)).

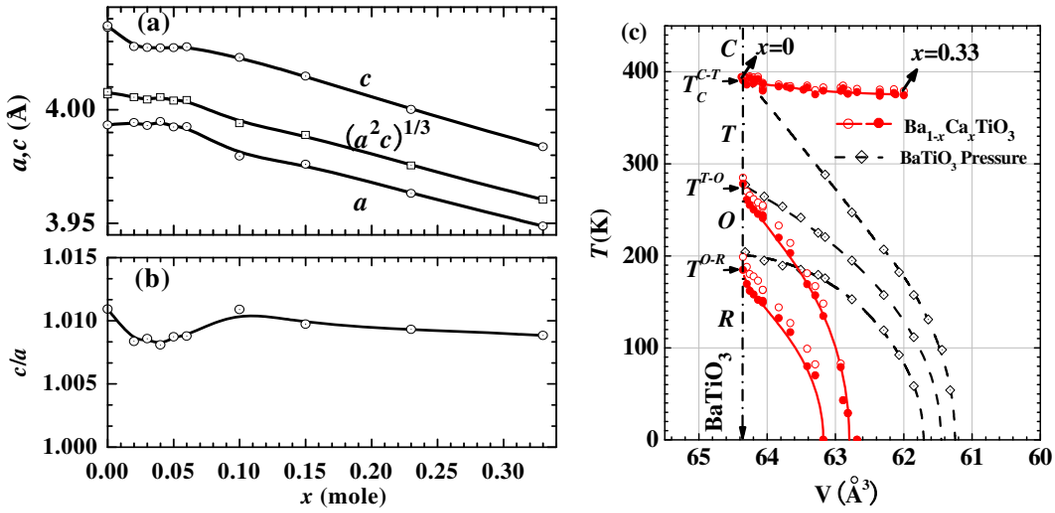

Figure 9. Change of (a) lattice constants and (b) tetragonality (*c*/*a*) of $(Ba_{1-x}Ca_x)TiO_3$ crystal. (c) Change of phase transition temperature as a function of unit cell volume (determined at room temperature);the hydrostatic pressure effect for pure $BaTiO_3$ is also shown for comparison.[7, 22, 23]

To examine the idea of Ca off-centering in the bulky Ba sites, we performed first principles calculations for this system.[7, 24] Since Ca substitution tends to stabilize the tetragonal structure, we focused on the calculations in this structure to get information about Ca displacement. The results are summarized in Fig. 10. As shown in Fig. 10(a), a Ti shift along the [001] direction leads to the stability of the tetragonal phase in $BaTiO_3$ (*x*=0). In our calculations for the substitution of Ca for Ba (*x*=1/8), we calculated the relative change in potential energy for various locations of the Ca ion, as shown schematically in Fig. 10(c). As shown in Fig. 11(d), a Ca off-centering shift results in the lowering of the potential energy of the system. This result clearly indicates that the Ca off-centering stabilizes the structure of the $(Ba_{1-x}Ca_x)TiO_3$ system. After tracing the variation of potential energy for moving Ca along various paths, we found that the most likely direction for a Ca shift is [113] since the potential energy is the lowest when Ca is shifted along this direction (Fig. 10(e)). The Ca-shift along the [113] direction seems to be incompatible with the tetragonal structure. However, if we consider the eight-site model

similar to that assumed for Ti displacement in $BaTiO_3$, then it becomes clear that Ca can displace along the equivalent directions [113], [1-13], [-113], [-1-13], or [11-3], [1-1-3], [-11-3], [-1-1-3]. The activation barrier for Ca moving between these equivalent states has been evaluated to be less than 3 meV. Therefore, thermal and spatial averaging among these states allows the preservation of the overall tetragonal symmetry detected from X-ray diffractions. It should be noted that the estimated displacement of Ca is approximately 0.1 Å (Fig. 10(d)), which is larger than the 0.05 Å shift of Ti in the tetragonal structure of $BaTiO_3$ (see Ref. 1 and Fig. 10(a)).

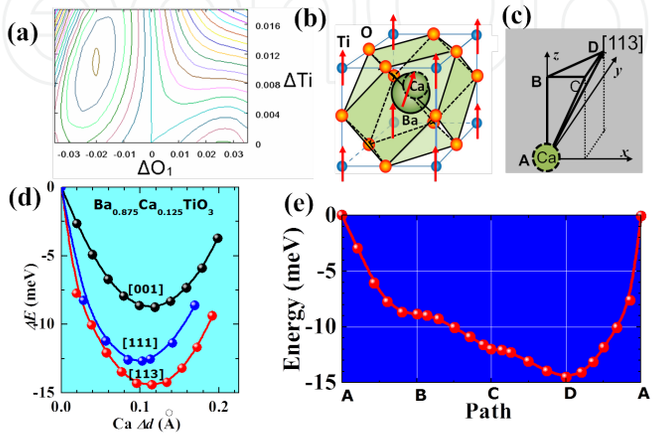

Figure 10. (a) Two-dimensional contour map of potential energy of $BaTiO_3$ as a function of Ti and O_1 displacement along the [001] direction of the polar *c*-axis. (b) Schematic of Ca off-centering in the bulky Ba sites of the perovskite structure, in which the atomic shifts are shown by the arrows. (c) Direction of Ca-shift for the first principles calculations of $Ba_{7/8}Ca_{1/8}TiO_3$. (d) Change of potential energy of $Ba_{7/8}Ca_{1/8}TiO_3$ along the [001], [111], and [113] directions. (e) Change of potential energy of $Ba_{7/8}Ca_{1/8}TiO_3$ along the path shown in (c).

2.5. Polarization and strain responses

For many technical applications, understanding the physical properties of a ceramics sample is of great importance. Figure 11 shows the variation of polarization, bipolar-, and unipolar-field-induced strains with the Ca substitution in the $(Ba_{1-x}Ca_x)TiO_3$ ceramics, which were measured at room temperature. One interesting finding is that the saturation polarization is nearly insensitive to the Ca substitution within the limit of solid solution[8] as shown in Fig. 11(a). This finding is predictable when considering the composition dependence of the tetragonality in the $(Ba_{1-x}Ca_x)TiO_3$ system. As shown in Fig. 9(b), the tetragonality has an approximate value of 1.01 within the solid solution limit. As mentioned above, the tetragonality of the ferroelectric perovskite oxides is predicted to be proportional to its spontaneous polarization by the theoretical calculations.[20, 21]

For the strain response under an electric field, with the exception of $BaTiO_3$ (x=0), $(Ba_{1-x}Ca_x)TiO_3$ ceramics show nearly the same level of strain response under the same electric field. For examples, the strain was observed to be approximately 0.08% for a unipolar field of 40 kV/cm, which corresponds to a level of piezoelectric response of 200 pm/V. The observation of the large strain response in $BaTiO_3$ is not surprising because its *T-O* phase transition is located at a temperature close to room temperature. Around the phase transition, a large response of physical properties generally occurs.

http://dx.doi.org/10.5772/61017

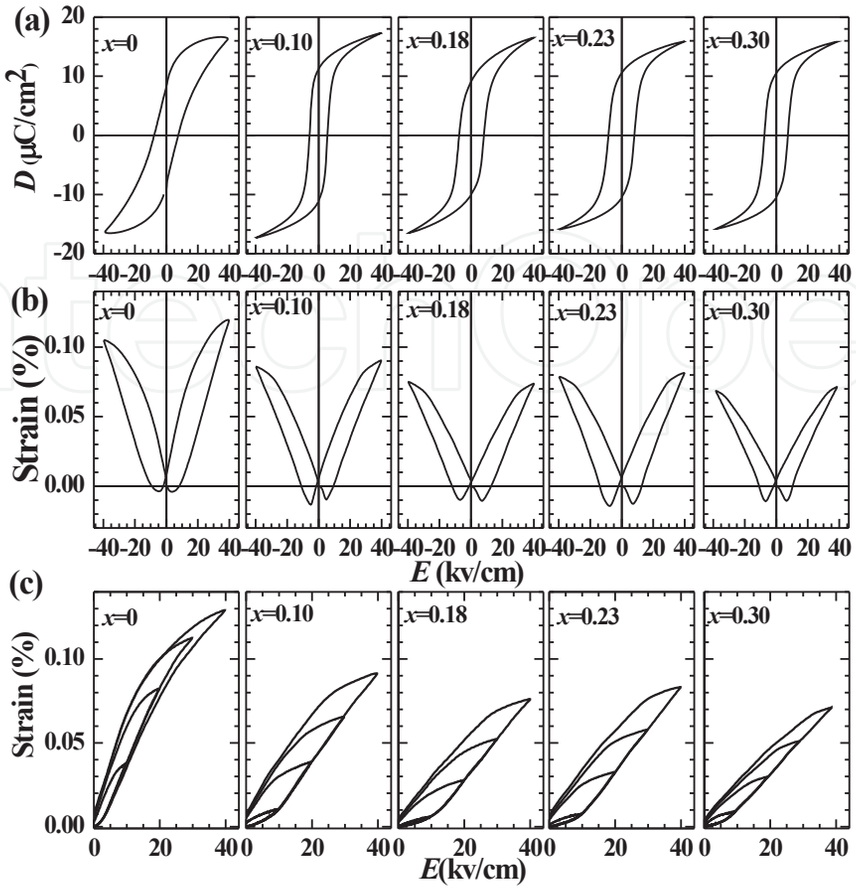

Figure 11. (a) Polarization, (b) bipolar-field and (c) unipolar-field strains under electric field in the $(Ba_{1-x}Ca_x)TiO_3$ ceramics.

3. Effects of Ca-substitution in the Ba(Ti,Zr)O_3 solid solution

To confirm the effects of Ca off-centering in Ba-based perovskite oxides, we also performed investigations on the system of Ba(Ti,Zr)O_3 solid solutions, which have been intensively studied since the mid-1950s.[25, 26] The most amazing finding in this system is that it demonstrates very large piezoelectric response, comparable to that of industrial PZT. A high electromechanical coupling factor of 74% and large piezoelectric coefficients of 340 pC/N under a high field were observed in this system.[27, 28] Another interesting thing in this system is that the *O*- or *R*-phase can be tuned to room temperature through controlling Zr substitution, which is of great significance for ferroelectric phase modification. However, as shown in the phase diagram reported by Kell and Hellicar (Fig. 12),[25] the problem of this system is that the Curie point decreases with the increase in the Zr concentration. For Zr concentrations larger than 20 mol%, the Curie point is reduced to a temperature lower than that at room temperature, leading to the disappearance of ferroelectricity in the crystal at room temperature. Here, we show that the Ca off-centering effects mentioned above can also be used to increase the Curie point of Ba(Ti,Zr)O_3 and enhance its electromechanical coupling effects through tuning the ferroelectric phase boundaries to room temperature.[9]

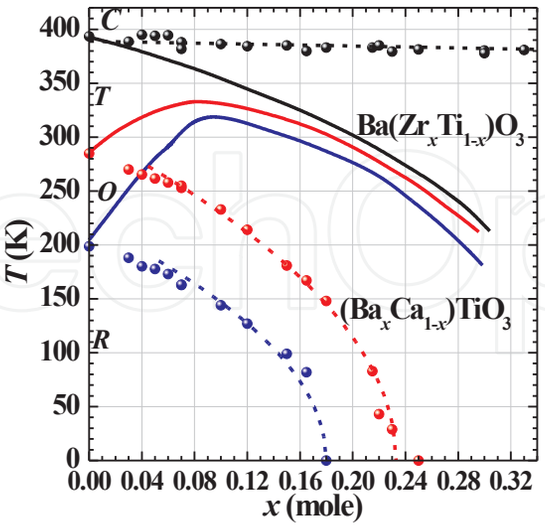

Figure 12. Phase diagram of $Ba(Ti_{1-x}Zr_x)O_3$ solid solutions proposed by Kell and Hellicar.[25] For comparison, the phase diagram of $(Ba_{1-x}Ca_x)TiO_3$ is also shown (solid circles).

3.1. Sample preparation

In our study, we selected a composition with a Zr concentration of 10 mol%, at which the three successive phases tend to approach each other as shown in Fig. 12. We prepared the $(Ba_{1-x}Ca_x)(Ti_{0.9}Zr_{0.1})O_3$ (BCTZO) ceramics by a solid-state reaction approach. Mixtures of $BaCO_3$, $CaCO_3$, ZrO_2, and TiO_2 were calcined at 1823 K for 3 h. The calcined powders were ground, pressed, and sintered at 1823 K for 5 h. The ceramic pellets were then electroplated with silver for electrical measurements.

3.2. Phase formation and structure transformation at room temperature

At the sintering temperature of 1823 K, a single phase of BCTZO was found to be formed within the composition range of $x \leq 0.18$ beyond which a non-ferroelectric phase with $CaTiO_3$-type orthorhombic structure occurs and coexist with the $BaTiO_3$-type ferroelectric phase. The phase equilibria of $(1-x)Ba(Zr_{0.1}Ti_{0.9})O_3$-$xCaTiO_3$ are very similar to those of $(1-x)BaTiO_3$-$xCaTiO_3$ reported by DeVries and Roy[15] as shown in Fig. 4(a). However, the solid solution limit of $(1-x)Ba(Zr_{0.1}Ti_{0.9})O_3$-$xCaTiO_3$ is approximately half that of $(1-x)BaTiO_3$-$xCaTiO_3$. This fact indicates that the substitution of Zr for Ti in $BaTiO_3$ will reduce the substitution amount of Ca for Ba.

At room temperature, BCTZO with x=0 has a ferroelectric rhombohedral structure as shown in phase diagram of Fig. 12. When Ba is substituted with Ca, the structure of BCTZO at room temperature was found to transform from *R*-phase to *O*-phase, and finally to *T*-phase with the increase in Ca concentration. Figure 13 shows the change of lattice parameters with Ca concentration for the BCTZO system. Similar to the unit cell of $(Ba_{1-x}Ca_x)TiO_3$ (Fig. 9(a)), the unit cell of BCTZO shrinks with the substitution of the smaller Ca for the bulky Ba, and its volume is reduced from 65.21 Å^3 for x=0 to 63.91 Å^3 for x=0.18. The ferroelectric lattice distortion

http://dx.doi.org/10.5772/61017

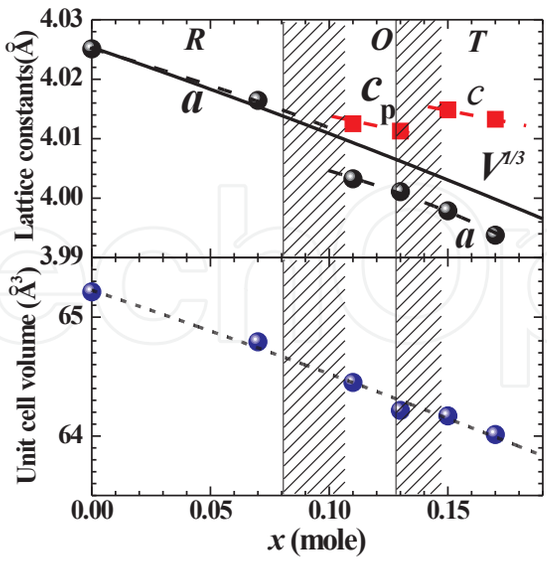

Figure 13. Change of the lattice parameters with composition at room temperature for the $(Ba_{1-x}Ca_x)(Ti_{0.9}Zr_{0.1})O_3$ system.

at room temperature is very small in the BCTZO solid solution. The distortion angles α in the *R*-phase and β of the monoclinic unit cell in the *O*-phase have deviations of only 0.01° and 0.1° from a right angle, respectively, while the tetragonality *c*/*a* has a value of 1.005 for x ≥ 0.15 in the *T*-phase.

3.3. Phase evolution with temperature

To understand the phase evolution in the BCTZO system, we have measured the temperature variation of dielectric permittivity for different Ca concentrations. The results are summarized in Fig. 14. As reported in many researches, three successive phase transitions are not easy to distinguish for BCTZO with *x*=0 because of the approach of the phase transition. However, these *C*-*T*, *T*-*O*, and *O*-*R* phase transitions as observed in $BaTiO_3$ are clearly demonstrated based on the temperature differentiations of dielectric permittivity shown in Fig. 14. Here, we used the peak of the temperature differentiation of dielectric permittivity to determine the transition temperature of *T*-*O* and *O*-*R* phase transitions.

The phase diagrams as functions of Ca concentration and unit cell volume are shown in Fig. 15(a) and (b), respectively. For comparison, a phase diagram of $(Ba_{1-x}Ca_x)TiO_3$ is also shown in the figure. There are several similarities between the BCTZO and $(Ba_{1-x}Ca_x)TiO_3$ systems: (a) Substitution of a smaller Ca for the bulky Ba shifts the *T*-*O* and *O*-*R* phase transitions to lower temperatures; in other words, Ca substitution results in the ferroelectric instability of the *O*- and *R*-phases in both systems. (B) By contrast, Ca substitution enhances the ferroelectric stability of the *T*-phase. (c) The chemical-pressure-induced shrink of the unit cell does not reduce the Curie point and weakens the ferroelectricity of both systems. These similarities between BCTZO and $(Ba_{1-x}Ca_x)TiO_3$ systems indicate that the Ca off-centering effects play a critical role in tuning the polarization states in these two systems.

However, there are also some differences between BCTZO and $(Ba_{1-x}Ca_x)TiO_3$ systems: (a) In $(Ba_{1-x}Ca_x)TiO_3$, the Curie point shows a slight decrease with the increase of Ca concentration, but it is increased in the BCTZO system. The Curie point is increased from 363 K for x=0 to 376 K for x=0.1, after which it seems to reach saturation with further substitution in BCZTO. (b) In $(Ba_{1-x}Ca_x)TiO_3$, the *O*- and *R*-phases completely disappear for Ca-substitution amount of x > 0.233, while in BCTZO, the disappearance of the *O*- and *R*-phases does not occur within the solid solution limit and the *R*-phase is still the ground state as occurs in pure $BaTiO_3$. These facts suggest that the contribution of Ca off-centering displacement to the whole spontaneous polarization in the BCTZO system may be greater than that in the $(Ba_{1-x}Ca_x)TiO_3$ system. This interpretation seems to be reasonable. Since $BaZrO_3$ is not ferroelectric even at zero Kelvin, and substitution of Zr for Ti reduces the ferroelectricity of $Ba(Ti,Zr)O_3$, in contrast to the large Ti displacement in the oxygen octahedron, the same level of Zr displacement is not expected to exist in the oxygen octahedron in $Ba(Ti,Zr)O_3$. Actually, this has been predicted from recent first-principles calculations, which indicates that Zr displacement is extremely small and has a value of about one-sixth of the Ti displacement at the lowest temperature in $Ba(Ti,Zr)O_3$.[29, 30] In contrast, as shown in Fig. 10. Ca displacement is predicted to have a value of two times the Ti displacement from first principles calculations. Therefore, in the BCTZO system, the polarization due to Ca-displacement is able to effectively compensate for the reduction of polarization from B-site atomic displacement due to the substitution of Zr for Ti, leading to the enhancement of ferroelectricity in the BCTZO system.

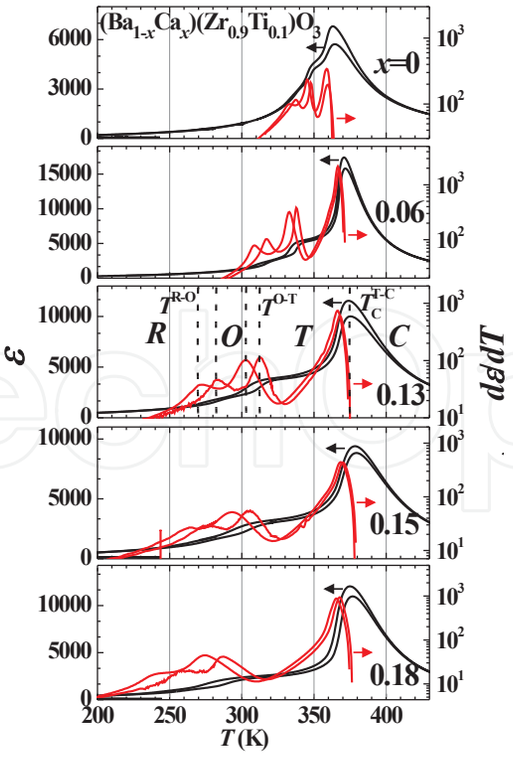

Figure 14. Temperature dependence of dielectric permittivity and its temperature differentiation in $(Ba_{1-x}Ca_x)(Ti_{0.9}Zr_{0.1})O_3$ ceramics.

http://dx.doi.org/10.5772/61017

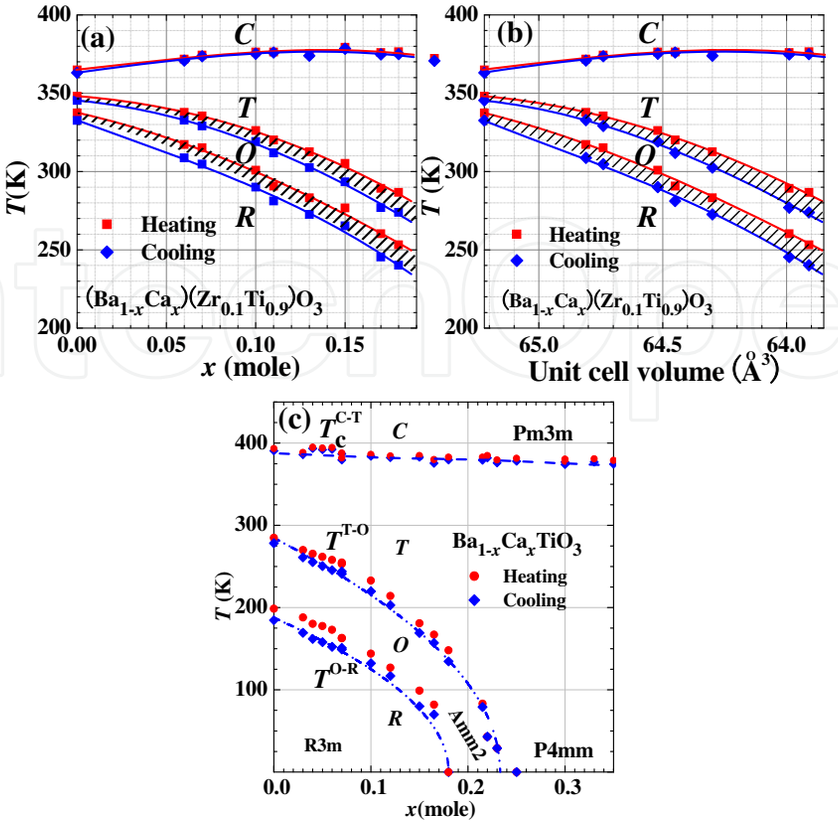

Figure 15. Phase diagrams of $(Ba_{1-x}Ca_x)(Ti_{0.9}Zr_{0.1})O_3$ solid solutions as functions of (a) composition and (b) unit cell volume. For comparison, the phase diagram of $(Ba_{1-x}Ca_x)TiO_3$ is also shown in (c).

3.4. Polarization and strain responses under an electric field

A *D-E* hysteresis loop of BCTZO is shown in Fig. 16(a). The remanent polarization was observed to have a value of approximately 10 μC/cm^2 for the ceramics samples at room temperature. It seems that there is a slight increase in the saturation polarization as the Ca concentration initially increases. This result is in agreement with the variation of Curie point with Ca concentration. It also seems that the coercive field becomes larger with the increase in Ca concentration.

On the other hand, the great enhancement of strain responses under an electric field is clearly observed for Ca-substituted ceramics as shown in Fig. 16(b) and (c). For example, the electric-field-induced strain for x=0 has a value of 0.054 % at E=10 kV/cm, for the same unipolar field, while it reaches a large value of 0.086% for x=0.10, which corresponds to an effective piezoelectric response of 860 pm/V. Figure 16(d) demonstrates the variation of this effective piezoelectric response around room temperature with Ca composition. It is clear that a large effective piezoelectric response with values higher than 800 pm/V has been observed in a wide composition range from x=0.06 to x=0.16 in the BCTZO ceramics, which is much larger than that obtained in the commercial PZT ceramics. Such extremely large electric-field-induced strain may be of great interest for the development of lead-free piezoelectric ceramics. As shown in Fig. 16(d), large electromechanical coupling effects occur around the *R-O* and *O-T*

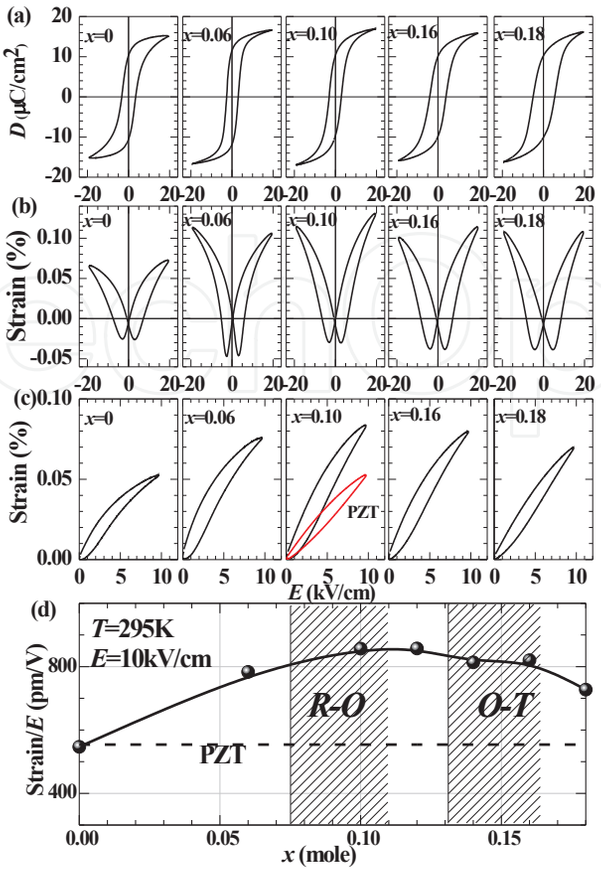

Figure 16. (a) Polarization, (b) bipolar-field, and (c) unipolar-field strain under electric field measured at T=295 K for $(Ba_{1-x}Ca_x)(Ti_{0.9}Zr_{0.1})O_3$ ceramics. For comparison, the response of commercially used PZT is also shown in (c). (d) Change of the strain at E=10kV/cm with composition.

phase boundaries. This indicates that the polymorphic phase transitions play a critical role in the large piezoelectric response in the BCTZO solid solution.

4. Summary

Ca off-centering was demonstrated to play a critical role in stabilizing the ferroelectric phase and tuning the polarization states in a $(Ba_{1-x}Ca_x)(Ti_{1-y}Zr_y)O_3$ system. Two typical cases, $((Ba_{1-x}Ca_x)TiO_3$ with y=0 and $(Ba_{1-x}Ca_x)(Ti_{0.9}Zr_{0.1})O_3$ with y=0.1), were studied. In both cases, atomic displacement due to Ca off-centering in the bulky Ba sites in the ABO_3 perovskite structure provides an approach to compensate for the reduction of ferroelectricity due to chemical pressure, leading to the maintenance of a nearly constant Curie point in the $(Ba_{1-x}Ca_x)TiO_3$ system and an increase in the Curie point in the $(Ba_{1-x}Ca_x)(Ti_{0.9}Zr_{0.1})O_3$ system. The Ca off-centering effects are commonly observed to lead to the shift of the *R–O* and *O–T* phase transitions toward lower temperatures and the ferroelectric stability of the *T*-phase, resulting in the occurrence of quantum phase transitions with interesting physics phenomena at low temperatures in the $(Ba_{1-x}Ca_x)TiO_3$ system and remarkable enhancement of electromechanical

http://dx.doi.org/10.5772/61017

coupling effects around room temperature in the $(Ba_{1-x}Ca_x)(Ti_{0.9}Zr_{0.1})O_3$ system over a large composition range.

Acknowledgements

We thank Prof. Shin-ya Koshihara & Dr. T. Shimizu of the Tokyo Institute of Technology, Mr. T. Kosugi & Prof. S. Tsuneyuki of the University of Tokyo, and Mr. Y. Kamai of the Shizuoka University for their collaboration in this work. We also thank the support from the Collaborative Research Project of the Materials and Laboratory, Tokyo Institute of Technology, and KAKENHI (15H02292 and 26620190).

Author details

Desheng Fu[1,2*] and Mitsuru Itoh[3]

*Address all correspondence to: fu.tokusho@shizuoka.ac.jp

1 Department of Engineering, Graduate School of Integrated Science & Technology, Shizuoka University, 3-5-1 Johoku, Hamamatsu, Japan

2 Department of Optoelectronics and Nanostructure Science, Graduate School of Science and Technology, 3-5-1 Johoku, Naka-ku, Hamamatsu, Japan

3 Materials and Structures Laboratory, Tokyo Institute of Technology, 4259 Nagatsuta, Yokohama, Japan

References

[1] Y. Shiozaki, E. Nakamura and T. Mitsui (eds). Ferroelectrics and related substances (Landolt-Bornstein, New Series, Group III, vol. 36, Pt. A1). Berlin: Springer; 2001.

[2] M. Zgonik, P. Bernasconi, M. Duelli, R. Schlesser, P. Günter, M. H. Garrett, D. Rytz, Y. Zhu and X. Wu. Dielectric, elastic, piezoelectric, electro-optic, and elasto-optic tensors of $BaTiO_3$ crystals. Phys. Rev. B 1994;50:5941. DOI: 10.1103/PhysRevB.50.5941.

[3] S.-E. Park and T. R. Shrout. Ultrahigh strain and piezoelectric behavior in relaxor based ferroelectric single crystals. J. Appl. Phys. 1997;82:1804. DOI: 10.1063/1.365983.

[4] R. Tazaki, D. Fu, M. Itoh, M. Daimon and S. Koshihara. Lattice distortion under an electric field in $BaTiO_3$ piezoelectric single crystal. J. Phys. Condens. Matter. 2009;21:215903. DOI: 10.1088/0953-8984/21/21/215903.

[5] J. Rodel, W. Jo, K. T. P. Seifert, E. M. Anton, T. Granzow and D. Damjanovic. Perspective on the development of lead-free piezoceramics. J. Am. Ceram. Soc. 2009;92:1153. DOI: 10.1111/j.1551-2916.2009.03061.x.

[6] D. Fu, M. Itoh and S. Koshihara. Crystal growth and piezoelectricity of $BaTiO_3$-$CaTiO_3$ solid solution. Appl. Phys. Lett. 2008;93:012904. DOI: 10.1063/1.2956400.

[7] D. Fu, M. Itoh, S. Koshihara, T. Kosugi and S. Tsuneyuki. Anomalous phase diagram of ferroelectric (Ba,Ca)TiO_3 single crystals with giant electromechanical response. Phys. Rev. Lett. 2008;100:227601. DOI: 10.1103/PhysRevLett.100.227601.

[8] D. Fu, M. Itoh and S. Koshihara. Invariant lattice strain and polarization in $BaTiO_3$–$CaTiO_3$ ferroelectric alloys. J. Phys. Condens. Matter. 2010;22:052204. DOI: 10.1088/0953-8984/22/5/052204.

[9] D. Fu, Y. Kamai, N. Sakamoto, N. Wakiya, H. Suzuki and M. Itoh. Phase diagram and piezoelectric response of $(Ba_{1-x}Ca_x)(Zr_{0.1}Ti_{0.9})O_3$ solid solution. J. Phys. Condens. Matter. 2013;25:425901. DOI: 10.1088/0953-8984/25/42/425901.

[10] A. von Hippel. Ferroelectricity, domain structure, and phase transitions of barium titanate. Rev. Mod. Phys. 1950;22:221. DOI: 10.1103/RevModPhys.22.221.

[11] W. Cochran. Crystal stability and the theory of ferroelectricity. Adv. Phys. 1960;9:387. DOI: 10.1080/00018736000101229.

[12] T. Mitsui and W. B. Westphal. Dielectric and x-ray studies of $Ca_xBa_{1-x}TiO_3$ and $Ca_xSr_{1-x}TiO_3$. Phys. Rev.1961;124:1354. DOI: 10.1103/PhysRev.124.1354.

[13] R. D. Shannon. Revised effective ionic radii and systematic studies of interatomic distances in halides and chalcogenides. Acta Crystallogr. Sect. A Cryst. Phys. Diffr. Theor. Gen. Crystallogr. 1976;32:751. DOI: 10.1107/S0567739476001551.

[14] T. Shimizu, D. Fu, H. Taniguchi, T. Taniyama and M. Itoh. Origin of the dielectric response in $Ba_{0.767}Ca_{0.233}TiO_3$. Appl. Phys. Lett. 2012;100:102908. DOI: 10.1063/1.3693524.

[15] R. C. DeVries and R. Roy. Phase Equilibria in the system $BaTiO_3$-$CaTiO_3$. J. Am. Ceram. Soc. 1955;38:142. DOI: 10.1111/j.1151-2916.1955.tb14918.x.

[16] Ch. Kuper, R. Pankrath and H. Hesse. Growth and dielectric properties of congruently melting $Ba_{1-x}Ca_xTiO_3$ crystals. Appl. Phys. A Mater. Sci. Process. 1997;65:301. DOI: 10.1007/s003390050583.

[17] T. Schneider, H. Beck and E. Stoll. Quantum effects in an n-component vector model for structural phase transitions. Phys. Rev. B 1976;13:1123. DOI: 10.1103/PhysRevB.13.1123.

[18] U. T. Hochli and L. A. Boatner. Quantum ferroelectricity in $K_{1-x}Na_xTaO_3$ and $KTa_{1-y}Nb_yO_3$. Phys. Rev. B 1979;20:266. DOI: 10.1103/PhysRevB.20.266.

[19] J. Iniguez and D. Vanderbilt. First-principles study of the temperature-pressure phase diagram of $BaTiO_3$. Phys. Rev. Lett. 2002;89:115503. DOI: 10.1103/PhysRevLett. 89.115503.

[20] J. B. Neaton, C. L. Hsueh and K. M. Rabe. Enhanced polarization in strained $BaTiO_3$ from first principles. arXiv:condmat/0204511;2002.

[21] S. Tinte, K. M. Rabe, and D. Vanderbilt. Anomalous enhancement of tetragonality in $PbTiO_3$ induced by negative pressure. Phys. Rev. B 2003;68:144105. DOI: 10.1103/ PhysRevB.68.144105.

[22] M. Malinowski, K. Lukaszewicz and S. Asbrink. The influence of high hydrostatic pressure on lattice parameters of a single crystal of $BaTiO_3$. J. Appl. Crystallogr. 1986;19:7. DOI: 10.1107/S0021889886090088.

[23] T. Ishidate, S. Abe, H. Takahashi and N. Mori. Phase Diagram of $BaTiO_3$. Phys. Rev. Lett. 1997;78:2397. DOI: 10.1103/PhysRevLett.78.2397.

[24] T. Kosugi, S. Tsuneyuki, D. Fu., M. Itoh, S. Koshihara. First-principles calculation of $Ba_{1-x}Ca_xTiO_3$ single crystal. Meeting abstract of the physical society of Japan 62(issue 2, part 4): 988. Hokkaido University. Sept. 22, 2007.

[25] R. C. Kell and N. J. Hellicar. Structural transitions in barium titanate-zirconate transducer materials. Acta Acustica united with Acustica. 1956;6:235.

[26] B. Jaffe, W. R. Cook, Jr. and H. Jaffe. Piezoelectric ceramics. London: Academic; 1967.

[27] P. W. Rehrig, S.-E. Park, S. Trolier-McKinstry, G. L. Messing, B. Jones and T. R. Shrout. Piezoelectric properties of zirconium-doped barium titanate single crystals grown by templated grain growth. J. Appl. Phys. 1999;86:1657. DOI: 10.1063/1.370943.

[28] Z. Yu, C. Ang, R. Guo and A. S. Bhalla. Piezoelectric and strain properties of $Ba(Ti_{1-x}Zr_x)O_3$ ceramics. J. Appl. Phys. 2002;92:1489. DOI: 10.1063/1.1487435.

[29] C. Laulhé, A. Pasture, F. Hippert and J. Kreisel. Random local strain effects in homovalent-substituted relaxor ferroelectrics: A first-principles study of $BaTi_{0.74}Zr_{0.26}O_3$. Phys. Rev. B 2010;82:13210. DOI: 10.1103/PhysRevB.82.132102.

[30] A. R. Akbarzadeh, S. Prosandeev, E. J. Walter, A. Al-Barakaty, and L. Bellaiche. Finite-temperature properties of Ba(Zr,Ti)O_3 relaxors from first principles. Phys. Rev. Lett. 2012;108:257601. DOI: 10.1103/PhysRevLett.108.257601.

IntechOpen